Published in final edited form as:
Ann Neurol. 2010 July ; 68(1): 81–91. doi:10.1002/ana.21994.

Thalamic sensitization transforms localized pain into widespread allodynia

Rami Burstein, PhD[1,2], **Moshe Jakubowski, PhD**[1], **Esther Garcia-Nicas, PhD**[1], **Vanessa Kainz**[1], **Zahid Bajwa, MD**[1], **Richard Hargreaves, PhD**[3], **Lino Becerra, PhD**[4], and **David Borsook, MD, PhD**[4]

[1]Department of Anesthesia and Critical Care, Beth Israel Deaconess Medical Center, Harvard Medical School, CLS-649, 330 Brookline Avenue, Boston, MA 02215

[2]Program in Neuroscience, Harvard Medical School, CLS-649, 330 Brookline Avenue, Boston, MA 02215

[3]Merck Research laboratories, WP-42-212, P.O. Box 4, 770 Sumneytown Pike, West Point, PA 19486

[4]P.A.I.N. Group, Department of Psychiatry, McLean Hospital, Harvard Medical School, 115 Mill Street, Belmont, MA 02478

Abstract

Objective—Focal somatic pain can evolve into widespread hypersensitivity to non-painful and painful skin stimuli (allodynia and hyperalgesia, respectively). We hypothesized that transformation of headache into whole-body allodynia/hyperalgesia during a migraine attack is mediated by sensitization of thalamic neurons that process converging sensory impulses from the cranial meninges and extracephalic skin.

Methods—Extracephalic allodynia was assessed using single unit recording of thalamic trigeminovascular neurons in rats and contrast analysis of BOLD signals registered in fMRI scans of patients exhibiting extracephalic allodynia.

Results—Sensory neurons in the rat posterior thalamus that were activated and sensitized by chemical stimulation of the cranial dura exhibited long-lasting hyperexcitability to innocuous (brush, pressure) and noxious (pinch, heat) stimulation of the paws. Innocuous, extracephalic skin stimuli that did not produce neuronal firing at baseline (e.g., brush) became as effective as noxious stimuli (e.g., pinch) in eliciting large bouts of neuronal firing after sensitization was established. In migraine patients, functional MRI assessment of blood oxygenation level-dependent (BOLD) signals showed that brush and heat stimulation at the skin of the dorsum of the hand produced larger BOLD responses in the posterior thalamus of subjects undergoing a migraine attack with extracephalic allodynia than the corresponding responses registered when the same patients were free of migraine and allodynia.

Interpretation—We propose that the spreading of multimodal allodynia and hyperalgesia *beyond* the locus of migraine headache is mediated by sensitized thalamic neurons that process nociceptive information from the cranial meninges together with sensory information from the skin of the scalp, face, body and limbs.

Correspondence – Rami Burstein, Department of Anesthesia and Critical Care, Beth Israel Deaconess Medical Center, CLS-649, 330 Brookline Avenue, Boston, MA 02215 Tel. (617) 735 2832; Fax (617) 735 2833; rburstei@bidmc.harvard.edu.

Introduction

Focal somatic pain can be associated with cutaneous allodynia (pain perception invoked by innocuous stimuli) and hyperalgesia (hypersensitivity to noxious stimuli) that spread beyond the original locus of pain.[1-3] Migraine-associated allodynia may develop at the site of the headache (typically around one eye) and spread throughout the face and scalp as well as the body and limbs.[4] Abnormal perception of cutaneous pain during a migraine attack is commonly invoked by mundane activities, such as combing one's hair, wearing tight cloths, shaving, or showering.[5-7] Indeed, pain thresholds to mechanical and thermal stimulation of cephalic and extracephalic skin, which are perfectly normal in the absence of migraine, drop significantly during migraine attacks that are associated with allodynia[7].

The initiation of headache during a migraine attack is believed to result from activation of a trigeminovascular pathway. The first-order neurons of the pathway are nociceptors that project from the trigeminal ganglion to the cranial meninges peripherally and to the spinal trigeminal nucleus (SpV) centrally. The second-order trigeminovascular neurons in the rat SpV process intracranial input from meningeal nociceptors and from extracranial skin and deep tissues around the eye.[8-10] Activation of such SpV neurons by nociceptive signals from the meninges is thought to produce the referred pain of migraine around the eye.[11,12] Sensitization of the first-order neurons provides the neural basis for the throbbing nature of migraine headache[13]. Subsequent sensitization of the second-order neurons[4,7,14] is associated with hyper-responsiveness to innocuous stimulation of the skin at the referred pain area.[10] Considering that the receptive fields of trigeminovascular SpV neurons are confined to one side of the head,[8,10,15] we reasoned that *extracephalic* allodynia during migraine reflects sensitization of higher-order trigeminovascular neurons that process bilateral sensory information from all segments of the spinal cord.

Evidence from several mammalian species has shown that posterior thalamic structures contain neurons that receive direct projections from trigeminovascular SpV neurons[16-18] and neurons that receive somatosensory information from all segments of the spinal cord.[19-21] We therefore hypothesized that the transformation of migraine headache into whole-body allodynia and hyperalgesia is mediated by thalamic neurons that integrate sensory information from the cranial dura mater and extracephalic skin. Using single-unit recording in the posterior thalamus of anesthetized rats, we identified individual dura-sensitive neurons that responded to innocuous and/or noxious stimuli from cephalic and extracephalic skin. Our goal was to determine whether brief chemical stimulation of the cranial dura would induce long-lasting sensitization in these neurons, such as to render them hyper-responsive to innocuous and noxious stimulation of extracephalic skin. To test whether extracephalic allodynia is associated with specific thalamic activation during migraine in humans, we employed functional magnetic-resonance imaging (fMRI) comparing responses elicited by innocuous and noxious skin stimuli in the presence and the absence of migraine.

Methods

Animals

Male Sprague-Dawley rats (350-400 g) were deeply anesthetized with urethane (1.2 g/kg i.p.). They were fitted with an intratracheal tube for artificial ventilation, mounted onto a stereotaxic frame, and received a bilateral craniotomy.

Single-unit recording in the rat

Trigeminovascular neurons having cephalic and extracephalic cutaneous receptive fields were studied *in vivo* using single unit recording in anesthetized male rats (1 unit/rat). A stainless-steel recording microelectrode (4-5 MΩ impedance) was lowered slowly toward

the Po or VPM in search for a single unit that responded to electrical and mechanical stimulation of the cranial dura, facial skin and paws. Each unit was tested to have exhibited discrete bursts of activity in response to electrical and mechanical stimulation of the dura and skin (increased mean spikes/sec of ≥25% compared to pre-stimulus activity). Repetitive electric shocks (0.8 msec, 0.5-3.0 mA, 1 Hz) were delivered to the dura overlying the contralateral (left) transverse sinus through a bipolar electrode. Indentation of the dura was applied with a von-Frey monofilament calibrated to a force of 3.63 g. Cutaneous receptive fields on the face (periorbital, vibrissal, lower lip), tail, and any one paw were mapped using repetitive electric shocks (0.5 msec, 10 mA, 1 Hz), innocuous mechanical stimuli (brush or pressure) and, if necessary, noxious stimuli (pinch or crash). Single-unit bursts of activity in response dural stimulation were isolated from background activity of neighboring units by fine-tuning the position the recording electrode tip, and adjusting the appropriate threshold for spike amplitude in the window discriminator. Isolated spikes were amplified and filtered in the window discriminator, and acquired for analysis using Biopac hardware and AcqKnowledge software (Biopac Systems Inc.).

Induction of central sensitization by dural stimulation in the rat

To induce central sensitization, the hotspot of the dural receptive field of each thalamic neuron was bathed for 5 min in IS (1 mM histamine, serotonin, bradykinin, 0.1 mM prostaglandin E2, 10 mM Hepes, pH 5.5) as described before.[22, 23] Control units received sham stimulation of the dura with SIF (135 mM NaCl, 5 mM KCl, 1 mM $MgCl_2$, 5 mM $CaCl_2$, 10 mM glucose, 10 mM Hepes, pH 7.2). Resting activity and neuronal responses to mechanical (brush, pressure, pinch) and thermal (heat, cold) stimulation of the contralateral face, the ipsilateral face, and contralateral paw were measured just before IS or SIF (baseline) and hourly thereafter. Ongoing neuronal activity was monitored over a 600-sec interval after the completion of each hourly stimulation cycle.

Stimulation of the rat skin

Mechanical stimuli (10 sec each) included brushing with a soft-bristle brush, pressing with a flat arterial clip, and pinching with a serrated arterial clip. Neuronal activity was monitored continuously, beginning 10 sec before brush and including ≥10-sec intervals after each stimulus to allow neuronal firing to return to baseline level (Fig. 2). Thermal stimulation consisted of gradually increasing skin temperature to 50 °C (face) or 55 °C (paw) and gradually lowering skin temperature to 0 °C (face, paw), using a 9×9 mm contact thermal probe (Yale University). Skin temperature was acclimated at 35 °C for 5 min before stimulation; ramped up (heat) or down (cold) at a rate of 1 °C/sec; maintained at target temperature for 5 sec; brought back to 35 °C at 1 °C/sec; and held at 35 °C for 300-600 sec after stimulation.

Neuronal activity was monitored continuously throughout the stimulus profile (Fig 2). As a rule, an increase in mean firing rate during a given stimulus by ≥25% above the pre-stimulus activity was considered to constitute a neuronal response to the respective stimulus. For thermal stimulation, the specific ramp temperature at which neuronal activity began to increase ≥25% above pre-stimulus level was referred to as the response threshold. Hypersensitivity to thermal stimuli was scored when response threshold shifted down ≥4°C (heat) or up ≥9°C (cold) after IS compared to baseline. Response magnitude and duration were measured from the onset of activity at the threshold temperature through the end of response (i.e., return to pre-stimulus level), or until the end of a 600-sec recording interval in those cases where neuronal firing remained elevated.

Localization of recording sites in the rat

At the end of each experiment, an electrolytic lesion was delivered through the tip of the recording electrode using direct anodal current (20 μA for 20 sec). Each rat was perfused with 10% formalin, and the brain was removed and stores at -20 °C. Coronal sections (50-μm thick) were collected serially using a freezing sliding microtome (Leica), and counterstained with neutral red for histological localization of lesion.

Human subjects

The study was approved by the McLean Hospital Institutional Review Board, in accordance with the Scientific and Ethical Guidelines for Human Research of the Helsinki Accord (http://ohsr.od.nih.gov/guidelines/helsinki.html). Included in the study were 18-55-year-old patients whose clinical history met the criteria for migraine with or without aura according to the International Headache Classification Committee.[24] They had 1-6 migraine attacks per month in the preceding 3 years, experienced migraine with cephalic and extracephalic allodynia,[4, 7] and were able to communicate clearly in English and provide an informed consent. Excluded from this study were subjects who had chronic daily headache, subjects with injuries and sensory disorders involving the peripheral or central nervous system (e.g., sensory neuropathies; chronic pain), and subjects using opiates or other analgesic drugs for reasons other than migraine.

Paradigm of fMRI

Each subject underwent two fMRI scans. For visit 1, subjects arrived at the MRI facility being free of migraine and allodynia for at least 7 days. For visit 2, subjects arrived 3-4 h after the onset of a unilateral, moderate-to-severe migraine headache, which they were required not to treat with any medication. In each visit, baseline cutaneous pain threshold to heat stimulation at the dorsum of the ipsilateral hand (side of headache) was measured before entering the MRI scanner, using QST as described in detail before[7]. Skin temperature was raised at 1 °C/sec from 32 °C (acclimation temperature) until the subject stopped the stimulator upon feeling local cutaneous pain at the site of the thermal probe (Medoc Advanced Medical Systems, Ramat Yishai, Israel). Thalamic activation was assessed using blood oxygenation level-dependent (BOLD) responses to skin stimulation in the absence of migraine and again during an untreated migraine attack. Assessment of pain level evoked by extracephalic brush and heat stimulation were determined in each visit before entering the MRI scanner.

Subjects were positioned in the scanner (3T Siemens Trio, Erlangen, Germany) with a quadrature head coil. MRI and fMRI scans were acquired first during brush stimulation and again during heat stimulation.[25,26] Brush stimulation was applied by stroking a pre-marked skin area with the soft side of a 1-cm wide piece of Velcro (1 stroke/sec). Brushing was delivered in a train of 3 repeated segments, each segment consisting of 30-sec rest (no stimulation) and 15-sec stimulation. Heat stimulation was custom-targeted for each subject to a temperature that was 1 °C above the pain threshold measured in the same subject just prior to entering the scanner in the respective visit. Heat stimulation during scanning was delivered in a train of 3 repeated segments, each segment consisting of 30-sec rest (32 °C) and 15-sec stimulation, using a 1.6×1.6 cm contact thermode (TSA-II, Medoc). Skin temperature was ramped up from 32 °C to the appropriate target level at 5 °C/sec, and lowered back to 32 °C at 4.5 °C/sec.

Upon completion of the scans in visit 2, patients were offered intravenous ketorolac (30 mg) to abort the attack, knowing from their previous history that they were unresponsive to triptans at this late stage of the attack.

Acquisition and analysis of fMRI data

Image acquisition, individual- and group-level image processing, region-of-interest analysis, and contrast analysis were performed as described before.[26] MRI images covering the whole brain were acquired interictally for anatomical orientation, using a 9-min-long sequence of magnetization prepared rapid gradient echo (MPRAGE) that yielded 128 sagittal slices (1.33-mm thick) at an in-plane resolution of 1 mm (256×256). A reduced MPRAGE sequence (2-min long, ten 3-mm-thick sagittal slices) was acquired ictally to render anatomical images for similar localization of functional images corresponding to the interictal images. Magnitude and phase images were acquired to unwarp functional scans, yielding thalamic slices corresponding in number and thickness to the fMRI scans. Functional scans covering the middle region of the cerebrum were acquired at an orientation matching the brainstem axis, yielding 33 coronal slices (3.5-mm thick) at in-plane resolution of 3.5 mm (64×64). Data acquisition was performed using a sequence of gradient echo (GE) echo planar imaging (EPI) with TE/TR=30/2500 msec. Each functional scan consisted of 74 volumes captured over 145 sec.

Functional MRI datasets were processed and analyzed using scripts from the Functional Magnetic Resonance Imaging of the Brain (FMRIB) Software Library (FSL) website at Oxford University (www.fmrib.ox.uk/fsl).[27] The initial two volumes were removed from each fMRI scan to allow for signal equilibration. The skull and extracranial structures were erased from the MRI and fMRI scans using the Brain Extraction Tool (BET) script. Motion detection and correction, using FMRIB Linear Image Registration Tool (MCFLIRT), indicated minimal motion during each functional scan (<2 mm). Functional scans were unwarped using FMRIB Utility for Geometrically Unwarping EPIs (FUGUE), and all volumes were normalized by the same mean-based intensity factor. Volumes were spatially smoothed using a 6-mm full-width filter set at half-maximum, and a 75 sec high-pass temporal filter.

First-level fMRI data analysis was performed for each subject using FMRI Expert Analysis Tool (FEAT) and FMRIB Improved Linear Model (FILM) version 5.4 with local autocorrelation correction.[28] Main explanatory variable (EV) for brush stimulation was constructed from a boxcar function convoluted with a standard hemodynamic response (FSL standard gamma function). Additional EV was generated for the temporal derivative of the main brush EV to account for small drifts in time.

For group-level analysis, individual statistics were fitted to a standard MNI brain, using FSL Linear Registration Tool (FLIRT). Group activation maps were pooled for each stimulus condition using fMRI Expert Analysis Tool (FEAT), applying a fixed-effects approach due to the small sample size. Contrast analysis was carried out in a pair-wise approach using FSL Feat tool.[27] Assumptions required for conventional threshold methods were not applicable, because the z-statistic values did not center at zero and did not exhibit a non-Gaussian distribution. Therefore, thresholds for statistical maps were determined using Gaussian Mixture Modeling (GMM), a multiple comparisons-based analysis, to identify categories of activated and deactivated voxels.[26,29,30]

The region of interest for data analysis was the thalamus. Group comparisons yielded images of specific activation clusters and tabulated coordinates of peak values within each cluster. For the purpose of presentation, thalamic fMRI signals were rendered over high-resolution (1×1×1 mm) standard MNI brain (FSL), using fixed-effects approach for a paired analysis of time courses obtained from averages across subjects and stimuli. Thalamic localization of the clusters and their peak foci was estimated using three atlases of the human brain.[31-33]

Statistical analysis

Data were analyzed using nonparametric statistics[34] and applying a two-tailed level of significance ($\alpha = 0.05$). For each group of trigeminovascular thalamic units, each measure of neuronal activity before IS (baseline) was compared to the *highest* corresponding measurement recorded after IS, using the Wilcoxon matched-pairs signed-ranks test. Similar analysis was used for the fMRI study to compare interictal *vs.* ictal measurements of heat pain threshold and psychophysical pain rating (VAS). Nominal data for independent samples were analyzed using the Chi-square test. Nominal data for related samples were analyzed using the McNemar test or the Binomial test, depending on sample size and expected frequencies.

Results

Characterization of trigeminovascular thalamic neurons

Forty-nine trigeminovascular neurons in the posterior thalamic region (1 neuron/rat) exhibited discrete responses to electrical and mechanical stimulation of the contralateral side of the cranial dura. Forty-one of those units exhibited bilateral cephalic *and* extracephalic receptive fields; in the remaining 8 units, cutaneous receptive fields were confined to the contralateral side of the face. Of the 49 units, 39 were challenged with 'inflammatory soup' (IS) applied for 5 min onto their exposed dural receptive field, whereas 10 units received sham stimulation of the dura with synthetic interstitial fluid (SIF). Neurons challenged with IS were divided into 3 subgroups on the basis of their responses to mechanical and thermal stimulation of the skin measured before and after IS.

Sensitized trigeminovascular units

Units that became hyper-responsive to skin stimulation *outside* the contralateral face (i.e., beyond the original cutaneous territory of trigeminovascular SpV neurons) were considered to be veritably and specifically sensitized by exposure of the dura to IS ($n = 24$). These neurons exhibited increased spontaneous activity (example – Fig. 1A) and increased responses to mechanical and thermal skin stimuli inside *and outside* the contralateral side of the head (examples – Fig. 2). Five units (21%) became sensitized to all three modalities (mechanical, heat, cold). Nine units (37%) became sensitized to two modalities (mechanical, heat). The remaining 10 units (42%) became sensitized to a single modality (6 – mechanical; 3 – heat; 1 – cold).

Ongoing firing rate increased significantly in sensitized neurons from 7.5 ± 1.4 spikes/sec at baseline to 18.5 ± 2.2 during the first 8 min after IS ($p < 0.0001$) and remained significantly elevated for several hours thereafter (Fig. 1B). Sensitized neurons significantly increased their response magnitude to cephalic *and* extracephalic brush (up 400% and 800%, respectively), pressure (up 400%) and pinch (up 100%) after IS compared to baseline (Fig. 2, Fig. 3A). Compared to baseline, the proportion of neurons responsive to skin stimuli after IS increased from 29 to 88% for cephalic brush ($p < 0.001$); from 8 to 50% for extracephalic brush ($p < 0.01$); from 58 to 88% for cephalic pressure ($p < 0.03$); and from 25 to 79% for extracephalic pressure ($p < 0.001$). Response magnitude to cephalic *and* extracephalic heat stimulation significantly doubled after IS compared to baseline (Fig. 2, Fig. 3A). Response threshold to cephalic heat stimulation dropped (i.e., sensitivity increased) from 47.9 ± 1.0 °C at baseline to 40.6 ± 1.0 °C after IS ($p < 0.02$) in 7/19 units tested (37%). Response threshold to extracephalic heat stimulation dropped from 52.3 ± 0.7 °C at baseline to 45.7 ± 1.4 °C after IS ($p < 0.004$) in 11/20 units tested (55%). Response magnitude to cephalic cold stimulation significantly doubled after IS compared to baseline, while responses to extracephalic cold stimulation remained unchanged (Fig. 3A). Response threshold to cephalic cold stimulation increased (i.e., sensitivity increased) from 8.3 ± 4.0 °C at baseline

to 27.3 ± 2.7 °C after IS ($p < 0.02$) in 7/20 units tested (35%). Response threshold to extracephalic cold stimulation remained unchanged after IS compared to baseline in 16/19 units that were tested.

The duration of neuronal firing elicited by noxious stimuli extended well beyond the interval of stimulation in the sensitized units (example – Fig. 2). Compared to baseline, response duration after IS increased significantly for cephalic pinch (up 9-fold) and for extracephalic pinch (up 5-fold) in all units that were tested, and for cephalic and extracephalic heat (up 4-fold) in 47% and 40% of the units tested, respectively (Fig. 4).

Non-sensitized trigeminovascular units

Neurons that became hyper-responsive to skin stimulation at the contralateral side of the face, *but nowhere else* ($n = 10$), were considered to be driven by increased input from SpV neurons that were rendered sensitized by exposing the dura to IS. These thalamic neurons significantly increased their ongoing firing rate from 8.9 ± 2.8 spikes/sec at baseline to 13.7 ± 4.0 during the first 8 min after exposing their dural receptive field to IS ($p < 0.03$). While ongoing activity remained relatively elevated thereafter, it was not significantly different from the baseline activity sampled before IS ($p > 0.1$; Fig. 1B). Non-sensitized units significantly increased their response magnitude to cephalic brush (up 400%), pressure and pinch (up 100%) compared to their responses at baseline (Fig. 3B). The proportion of neurons responsive to tactile stimulation of the facial skin increased from 30% at baseline to 70% after IS for brush, and from 50 to 80% for pressure. Response magnitudes to stimulation of the facial skin increased after IS by 200 for heat and 300% for cold compared to baseline (Fig. 3B). Heat threshold measured before and after IS remained unchanged (46.3 ± 1.4 *vs.* 47.2 ± 1.4 °C) in the 8 units that were tested. Cold threshold increased in 5 of those neurons from 4.8 ± 4.8 at baseline to 26.2 ± 4.7 °C after IS ($p < 0.05$). Compared to baseline, response duration after IS increased >10-fold for cephalic pinch in 3/3 units tested, and >3-fold for cephalic heat in 3/7 units tested.

Unaffected trigeminovascular units

In this group of neurons ($n = 5$), the magnitude, threshold, or duration of responses to cephalic and extracephalic skin stimuli did not increase after IS compared to baseline (Fig. 3C). Ongoing neuronal activity was 8.8 ± 3.3 spikes/sec at baseline, 15.4 ± 5.2 during the first 8 min after IS ($p > 0.5$), and remained essentially unchanged from baseline thereafter ($p > 0.1$; Fig. 1B).

Control units

In this group of neurons, sham stimulation of the dura with SIF did not result in increased responsiveness to cephalic or extracephalic skin stimuli (Fig. 3D). On the contrary, response magnitude to cephalic brush, pressure and heat, as well as extracephalic heat, *decreased* significantly over time compared to baseline (Fig. 3D). Ongoing neuronal activity remained unchanged throughout the experiment (Fig. 1B). Response duration to cephalic heat stimulation decreased significantly from 22.3 ± 4.5 spikes/sec before SIF to 8.8 ± 2.3 after SIF ($p < 0.03$).

Histological localization of recording sites (Fig. 5)

Lesions marking the recording sites were located in the posterior region of the thalamus. Units challenged with IS were localized in a mediodorsal cluster ($n = 25$) or a ventrobasal cluster ($n = 14$). The mediodorsal cluster included the Po, the lateral posterior (LP) and lateral dorsal (LD) thalamic nuclei, the granular triangular part of Po (PoT), and subparafascicular nucleus (SPF). The ventrobasal cluster included the main body of VPM,

and the caudal part of VPL. Control units were equally divided between the two clusters. Of the 41 dura-sensitive neurons that exhibited both cephalic *and* extracephalic receptive fields at baseline, 26 (63%) were located mediodorsally and 15 (37%) ventrobasally. Of the 8 neurons whose cutaneous receptive fields at baseline were confined to the contralateral side of the face, 2 were located mediodorsally and 6 ventrobasally. The ratio of distribution between the mediodorsal and the ventrobasal clusters was 16:8 for the sensitized units, 5:5 for the non-sensitized units, and 4:1 for the unaffected units ($p > 0.6$).

fMRI contrast analysis in the presence vs. absence of migraine

On the basis of the findings in the rat, we employed fMRI to assess whether mechanical and thermal skin stimuli elicited specific thalamic activation during migraine attacks associated with extracephalic allodynia. Of 20 recruits with episodic migraine, 15 met the criteria for migraine with extracephalic allodynia, and 8 of those completed the study as described below.

Gentle brushing of the skin at the dorsum of the hand ipsilateral to the side of headache was perceived to be innocuous in the absence of migraine and painful during a migraine attack (Supplementary Figure A). During fMRI scanning, each patient received heat stimulations delivered at 1 °C above the pain threshold measured in the same subject just before entering the scanner. Tweaking the stimulus temperature according to the individual threshold established in each visit resulted in perceived cutaneous pain that was rated similarly during migraine and interictally (Supplementary Figure B). Pain threshold to heat stimulation at the dorsum of the hand dropped significantly from 48.4 ± 0.7 interictally to 43.4 ± 1.0 °C during migraine ($p = 0.0116$), as determined by QST (Supplementary Figure C).

Thalamic BOLD signals induced by brush and heat stimulation of the hand were significantly larger during migraine attacks with extracephalic allodynia than the corresponding BOLD signals registered when the same patients were free of both migraine and allodynia (Fig. 6). Contrast analysis of ictal *vs.* interictal activation patterns induced by heat stimulation of the hand (Fig. 6A) were localized *contralaterally* to the side of headache in the pulvinar, parafascicular, (PF), medial dorsal (MD) and LP, and *ipsilaterally* in PF, VPL, centrolateral nucleus (CL), centromedian (CM), MD and LKP and VA. Activation patterns induced by brush stimulation of the hand during migraine (Fig. 6C) were mapped *contralaterally* to the pulvinar, CM, VL, VA and MD, and *ipsilaterally* to the pulvinar, PF, VPL, CM, VL, VA and MD.

Discussion

To understand the transformation of migraine headache into widespread, cephalic and extracephalic allodynia, we studied the effects of mechanical and thermal skin stimuli on activity of third-order trigeminovascular neurons in the rat thalamus, and on thalamic activation registered by fMRI during migraine in human subjects. In the rat thalamus, trigeminovascular neurons that processed converging sensory information from the cranial meninges and from the skin were activated by briefly exposing their dural receptive field to IS, and exhibited long-lasting hyperexcitability to cephalic and extracephalic skin stimuli. Functional MRI with patients undergoing migraine with whole-body allodynia yielded evidence for acute thalamic activation in response to extracephalic brush and heat stimuli. Collectively, the results suggest that the spread of multimodal allodynia and hyperalgesia *outside* the original site of migraine headache is associated with sensitization of third-order thalamic neurons that process mechanical and thermal sensory information converging from the meninges, head, body and limbs.

The neural mechanisms by which trigeminovascular thalamic neurons become sensitized may involve sequential sensitization of first-, second-order trigeminovascular neurons or, alternatively, indirect activation through pain modulatory neurons in the brainstem.[35,36] According to the first scenario, a barrage of incoming signals from meningeal nociceptors sensitizes the trigeminovascular neurons in SpV which, in turn, bombard the trigeminovascular neurons in the thalamus and render them sensitized. According to the second scenario, second- and third-order trigeminovascular neurons become sensitized independently of each other by activated pain-facilitating "on" cells in the rostral ventromedial medulla (RVM) with descending projections to SpV and the spinal cord, and ascending projections to the thalamus.[37] Activation of pain-facilitating "on" cells that ascend to the thalamus may alter the excitability of third-order trigeminovascular neurons with whole body receptive fields and render them sensitized. Alternatively, activation of pain-facilitating "on" cells that descend to the spinal cord should produce hyperexcitability in nociceptive neurons at all spinal dermatomes, which can exaggerate the transmission of pain to the thalamus. Future experiments will have to determine whether or not the transmission of pain signals in the lumbar cord is enhanced following administration of inflammatory mediators on the rat dura.

Hyperexcitability of thalamic units to skin stimuli within the contralateral side of the head was attributed to sensitization of trigeminovascular neurons in the SpV.[10] On the other hand, extracephalic hyperexcitability (as well as hyperexcitability involving the ipsilateral side of the head) was attributed to thalamic sensitization, because it spread outside the cutaneous territory of SpV neurons, and because the experimental paradigm of sensitization (exposing the dura to IS) does not involve activation of pathways outside the trigeminovascular system. Unlike non-sensitized thalamic units driven by SpV sensitization, thalamic neurons that became sensitized in their own right increased their ongoing firing rate significantly and exhibited hyper-responsiveness (increased response magnitude) and hypersensitivity (lower response threshold) to extracephalic stimuli (mechanical and thermal). In such units, innocuous extracephalic skin stimuli that did not induce neuronal firing before sensitization (e.g., brush) became as effective as noxious stimuli (e.g., pinch) in triggering large bouts of activity after sensitization was established. Many of the sensitized thalamic neurons exhibited protracted firing in response to noxious extracephalic stimuli.

The presence of dura-sensitive neurons in the rat Po and VPM agrees with rat and cat studies,[38-41] and is in line with evidence that both nuclei receive direct projections from trigeminovascular neurons in laminae I and V of the SpV.[10] In agreement with other studies,[38-41] we identified dura-sensitive VPM neurons whose cutaneous receptive fields were confined to the contralateral face. Based on the somatotopic organization[19-21,42-44] and the afferent connections of the Po and VPM,[17,18,42,45-47] we expected that neurons with large, bilateral cephalic *and* extracephalic receptive fields would be present in the Po, but absent from the VPM. In the cat, trigeminovascular neurons having cephalic and extracephalic sensory receptive fields were identified in the Po but not in VPM.[39] In the rat, on the other hand, we found many such neurons not only in the Po, but also in the VPM, LD and LP. Species and methodological differences aside, the anatomical organization of trigeminovascular thalamic neurons that process extracephalic sensory information appears to diverge from the strict somatotopic thalamic organization characteristic of non-trigeminovascular somatosensory neurons.

Consistent with the findings in the rat, patients undergoing a migraine attack with extracephalic allodynia responded to extracephalic skin stimuli with specific BOLD signals in the posterior thalamus. It remains to be shown, however, whether or not migraine without extracephalic allodynia is associated with enhanced BOLD signals in the posterior thalamus. It should be noted that comparative neuroanatomy of the thalamus is subject to considerable

species differences in terms of nomenclature systems, anatomical description, and anatomical connections.[31,48,49] With those caveats in mind, the localization of sensitized trigeminovascular neurons in the rat mediodorsal region of the thalamus (Po, LD, LP) may best correspond to the BOLD signals induced in the rostral part of the human pulvinar by extracephalic heat stimulation during migraine. Considering that the pulvinar, which is absent from the rat thalamus, is presumed to have evolved from the LP of lower mammals,[49] our findings would suggest that the so-called 'pulvinar-LP complex' is equipped to process not only visual signals,[50,51] but also nociceptive information from large extracephalic skin areas. The localization of sensitized trigeminovascular neurons in the rat ventrobasal thalamus is consistent with the BOLD signals induced in the human VPL by extracephalic brush and heat stimulation during migraine. The induction of BOLD signals in the CL and CM-PF complex by extracephalic heat stimulation during migraine is consistent with the presence of nociceptive neurons with whole-body receptive fields in these intralaminar nuclei.[52] Whether such intralaminar neurons also process nociceptive information from the meninges and, thus, play a role in migraine pathophysiology remains to be determined. BOLD signals induced in response to extracephalic skin stimuli in other thalamic nuclei (MD, VL, VA) may not be specific to migraine, as these nuclei have been shown to be activated directly by extracephalic nociception.[53,54]

In summary, we identified trigeminovascular neurons in the rat thalamus that became sensitized to innocuous and noxious stimulation of extracephalic skin after their initial activation by chemical stimulation of the cranial dura mater. In human subjects, thalamic BOLD signals elicited by extracephalic skin stimuli were greater during migraine than interictally. Taken together, these findings suggest that sensitization of trigeminovascular thalamic neurons propels the transformation of migraine headache into multimodal allodynia and hyperalgesia throughout the body.

Supplementary Material

Refer to Web version on PubMed Central for supplementary material.

Acknowledgments

This research was supported by NIH grants NS-051484 (RB) and NS-056195 (DB, RB, LB), and K24 064050 (DB), and by a grant from Merck & Co. We thank Lauren Nutile for her assistance in the fMRI study.

References

1. Sieweke N, Birklein F, Riedl B, et al. Patterns of hyperalgesia in complex regional pain syndrome. Pain. 1999; 80:171–177. [PubMed: 10204729]
2. Vierck CJ Jr. Mechanisms underlying development of spatially distributed chronic pain (fibromyalgia). Pain. 2006; 124:242–263. [PubMed: 16842915]
3. O'Neill S, Manniche C, Graven-Nielsen T, Arendt-Nielsen L. Generalized deep-tissue hyperalgesia in patients with chronic low-back pain. European journal of pain (London, England). 2007; 11:415–420.
4. Burstein R, Cutrer FM, Yarnitsky D. The development of cutaneous allodynia during a migraine attack: clinical evidence for the sequential recruitment of spinal and supraspinal nociceptive neurons in migraine. Brain. 2000; 123:1703–1709. [PubMed: 10908199]
5. Liveing, E. On megrim, sick headache. Arts & Boeve Publishers; Nijmegen: 1873.
6. Wolff HG, Tunis MM, Goodell H. Studies on migraine. Arch. Internal Medicine. 1953; 92:478–484.
7. Burstein R, Yarnitsky D, Goor-Aryeh I, et al. An association between migraine and cutaneous allodynia. Annals Neurol. 2000; 47:614–624.

8. Davis KD, Dostrovsky JO. Responses of feline trigeminal spinal tract nucleus neurons to stimulation of the middle meningeal artery and sagittal sinus. Journal of Neurophysiology. 1988; 59:648–666. [PubMed: 3351579]
9. Strassman AM, Mason P, Moskowitz M, Maciewicz RJ. Response of medullary trigeminal neurons to electrical stimulation of the dura. Brain research. 1986; 379:242–250. [PubMed: 3742223]
10. Burstein R, Yamamura H, Malick A, Strassman AM. Chemical stimulation of the intracranial dura induces enhanced responses to facial stimulation in brain stem trigeminal neurons. Journal of Neurophysiology. 1998; 79:964–982. [PubMed: 9463456]
11. Penfield, w. A contribution to the mechanism of intracranial pain. Assoc. Res. Nerv. Dis. Proc. 1935; 15:399–416.
12. Ray BS, Wolff HG. Experimental studies on headache. Pain-sensitive structures of the head and their significance in headache. Arch. Surg. 1940; 41:813–856.
13. Strassman AM, Raymond SA, Burstein R. Sensitization of meningeal sensory neurons and the origin of headaches. Nature. 1996; 384:560–564. [PubMed: 8955268]
14. Burstein R. Deconstructing migraine headache into peripheral and central sensitization. Pain. 2001; 89:107–110. [PubMed: 11166465]
15. Ebersberger A, Ringkamp M, Reeh PW, Handwerker HO. Recordings from brain stem neurons responding to chemical stimulation of the subarachnoid space. Journal of Neurophysiology. 1997; 77:3122–3133. [PubMed: 9212262]
16. Burton H, Craig ADJ, Poulos DA, Molt JT. Efferent projections from temperature sensitive recording loci within the marginal zone of the nucleus caudalis of the spinal trigeminal complex in the cat. Journal of Comparative Neurology. 1979; 183:753–778. [PubMed: 762271]
17. Berkley KJ. Spatial relationships between the terminations of somatic sensory and motor pathways in the rostral brainstem of cats and monkeys. I. Ascending somatic sensory inputs to lateral diencephalon. Journal of Comparative Neurology. 1980; 193:283–317. [PubMed: 7430431]
18. Cliffer KD, Burstein R, Giesler GJ Jr. Distributions of spinothalamic, spinohypothalamic, and spinotelencephalic fibers revealed by anterograde transport of PHA-L in rats. J Neurosci. 1991; 11:852–868. [PubMed: 1705972]
19. Poggio GF, Mountcastle VB. The functional properties of ventrobasal thalamic neurons studied in unanesthetized monkeys. Journal of Neurophysiology. 1963; 26:775–806. [PubMed: 14065328]
20. Chiaia NL, Rhoades RW, Fish SE, Killackey HP. Thalamic processing of vibrissal information in the rat: II. Morphological and functional properties of medial ventral posterior nucleus and posterior nucleus neurons. Journal of Comparative Neurology. 1991; 314:217–236. [PubMed: 1723993]
21. Apkarian AV, Shi T. Squirrel monkey lateral thalamus. I. Somatic nociresponsive neurons and their relation to spinothalamic terminals. J Neurosci. 1994; 14:6779–6795. [PubMed: 7965079]
22. Steen KH, Reeh PW, Anton F, Handwerker HO. Protons selectively induce lasting excitation and sensitization to mechanical stimulation of nociceptors in rat skin, in vitro. J Neurosci. 1992; 12:86–95. [PubMed: 1309578]
23. Steen KH, Steen AE, Reeh PW. A dominant role of acid pH in inflammatory excitation and sensitization of nociceptors in rat skin, in vitro. J Neurosci. 1995; 15:3982–3989. [PubMed: 7751959]
24. The International Classification of Headache Disorders. Second Edition. Vol. 24. Cephalalgia: 2004. p. 1-160.
25. Becerra L, Breiter HC, Wise R, et al. Reward circuitry activation by noxious thermal stimuli. Neuron. 2001; 32:927–946. [PubMed: 11738036]
26. Moulton EA, Pendse G, Morris S, et al. Capsaicin-induced thermal hyperalgesia and sensitization in the human trigeminal nociceptive pathway: an fMRI study. NeuroImage. 2007; 35:1586–1600. [PubMed: 17407825]
27. Smith SM, Jenkinson M, Woolrich MW, et al. Advances in functional and structural MR image analysis and implementation as FSL. NeuroImage. 2004; 23(Suppl 1):S208–219. [PubMed: 15501092]
28. Woolrich MW, Ripley BD, Brady M, Smith SM. Temporal autocorrelation in univariate linear modeling of FMRI data. NeuroImage. 2001; 14:1370–1386. [PubMed: 11707093]

29. Becerra L, Morris S, Bazes S, et al. Trigeminal neuropathic pain alters responses in CNS circuits to mechanical (brush) and thermal (cold and heat) stimuli. Journal of Neuroscience. 2006; 26:10646–10657. [PubMed: 17050704]
30. Woolrich MW, Behrens TE, Beckmann CF, Smith SM. Mixture models with adaptive spatial regularization for segmentation with an application to FMRI data. IEEE transactions on medical imaging. 2005; 24:1–11. [PubMed: 15638182]
31. Schaltenbrand, G.; Wahren, W. Atlas for Stereotaxy of the Human Brain. Thieme; stutgart: 1977.
32. Hirai T, Jones EG. Distribution of tachykinin- and enkephalin-immunoreactive fibers in the human thalamus. Brain research. 1989; 14:35–52.
33. Mai, JK.; Paxinos, G.; Voss, T. Atlas of the Human Brain. 3rd ed.. Academic Press; New York: 2008.
34. Siegel, S. Nonparametric Statistics for the Behavioral Sciences. McGrow-Hill Kogakusha; Tokyo: 1956. p. 312
35. Weiller C, May A, Limmroth V, et al. Brain stem activation in spontaneous human migraine attacks. Nat Med. 1995; 1:658–660. [PubMed: 7585147]
36. Bahra A, Matharu MS, Buchel C, et al. Brainstem activation specific to migraine headache. Lancet. 2001; 357:1016–1017. [PubMed: 11293599]
37. Edelmayer RM, Vanderah TW, Majuta L, et al. Medullary pain facilitating neurons mediate allodynia in headache-related pain. Ann Neurol. 2009; 65:184–193. [PubMed: 19259966]
38. Davis KD, Dostrovsky JO. Properties of feline thalamic neurons activated by stimulation of the middle meningeal artery and sagittal sinus. Brain research. 1988; 454:89–100. [PubMed: 3409027]
39. Zagami AS, Lambert GA. Stimulation of cranial vessels excites nociceptive neurones in several thalamic nuclei of the cat. Experimental Brain Research. 1990; 81:552–566.
40. Angus-Leppan H, Olausson B, Boers P, Lambert GA. Convergence of afferents from superior sagittal sinus and tooth pulp on cells in the thalamus of the cat. Cephalalgia. 1995; 15:191–199. [PubMed: 7553808]
41. Shields KG, Goadsby PJ. Propranolol modulates trigeminovascular responses in thalamic ventroposteromedial nucleus: a role in migraine? Brain. 2005; 128:86–97. [PubMed: 15574468]
42. Gauriau C, Bernard JF. A comparative reappraisal of projections from the superficial laminae of the dorsal horn in the rat: the forebrain. Journal of Comparative Neurology. 2004; 468:24–56. [PubMed: 14648689]
43. Curry MJ. The exteroceptive properties of neurones in the somatic part of the posterior group (PO). Brain research. 1972; 44:439–462. [PubMed: 5075704]
44. Brinkhus HB, Carstens E, Zimmermann M. Encoding of graded noxious skin heating by neurons in posterior thalamus and adjacent areas in the cat. Neurosci Lett. 1979; 15:37–42. [PubMed: 530514]
45. Jones EG, Burton H. Cytoarchitecture and somatic sensory connectivity of thalamic nuclei other than the ventrobasal complex in the cat. Journal of Comparative Neurology. 1974; 154:395–432. [PubMed: 4132971]
46. Willis WD, Zhang X, Honda CN, Giesler GJ. Projections from the marginal zone and deep dorsal horn to the ventrobasal nuclei of the primate thalamus. Pain. 2001; 92:267–276. [PubMed: 11323148]
47. Zhang X, Giesler GJ Jr. Response characterstics of spinothalamic tract neurons that project to the posterior thalamus in rats. Journal of Neurophysiology. 2005; 93:2552–2564. [PubMed: 15845999]
48. Hirai T, Jones EG. A new parcellation of the human thalamus on the basis of histochemical staining. Brain research. 1989; 14:1–34.
49. Percheron, G. Thalamus.. In: Paxinos, G.; Mai, JK., editors. The Human Nervous System. Elsevier Academic Press; San Diego, CA: 2004. p. 592-675.
50. The pulvinar-LP complex. Charles C. Thomas; Springfield, Illinois: 1974.
51. Chalfin BP, Cheung DT, Muniz JA, et al. Scaling of neuron number and volume of the pulvinar complex in New World primates: comparisons with humans, other primates, and mammals. The Journal of comparative neurology. 2007; 504:265–274. [PubMed: 17640049]

52. Willis, JWD.; Westlund, KN. Pain system.. In: Paxinos, G.; Mai, JK., editors. The Human Nervous System. Elsevier Academic Press; San Diego, CA: 2004. p. 1125-1170.

53. Singer T, Seymour B, O'Doherty J, et al. Empathy for pain involves the affective but not sensory components of pain. Science (New York, N.Y. 2004; 303:1157–1162.

54. Becerra LR, Breiter HC, Stojanovic M, et al. Human brain activation under controlled thermal stimulation and habituation to noxious heat: an fMRI study. Magn Reson Med. 1999; 41:1044–1057. [PubMed: 10332889]

55. Paxinos, G.; Watson, C. The Rat Brain in Stereotaxic Coordinates. Fourth ed. Academic Press; Orlando: 1998.

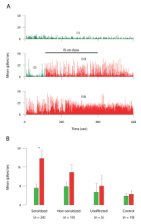

Fig. 1.

Long-lasting increase in ongoing activity of sensitized thalamic neurons after exposing their dural receptive fields to IS. (*A*) Examples of neuronal firing recorded at baseline (top), during a 5-min stimulation of the dura with IS (middle), and 3 h later (bottom). Numbers in parentheses indicate mean spikes/sec before (green) and after IS (red). Bin width: 500 msec. (*B*) Ongoing firing rate before (green) and after IS (red). Each bar represents mean ± SEM activity calculated from a 600-sec interval of continuous recording. Red bars represent and highest mean activity recorded at any one hourly time point after IS. Note that the increase in ongoing activity was significant in the group of sensitized units ($p < 0.0001$, Wilcoxon test), but not in the other groups.

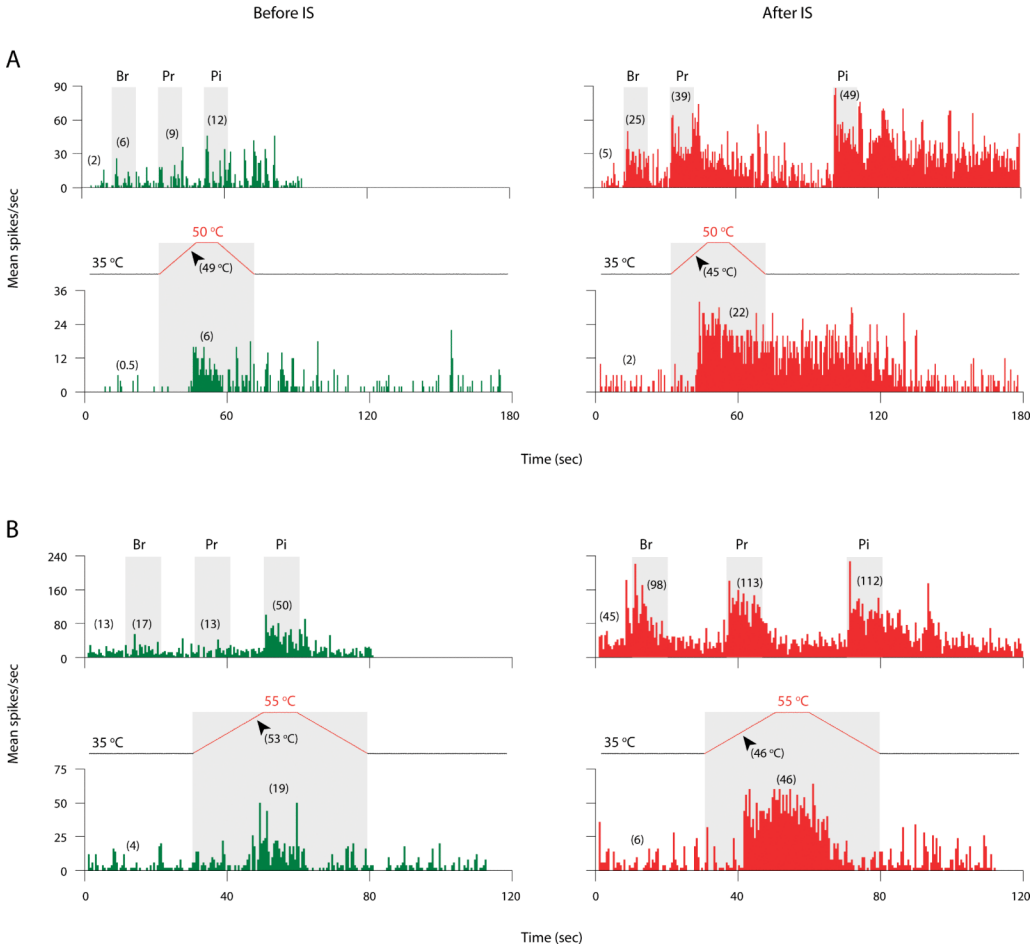

Fig. 2.

Increased responses of sensitized thalamic neurons to cephalic (*A*) and extracephalic (*B*) skin stimuli after exposing their dural receptive fields to IS. Shown are examples of neuronal responses to brush (Br), pressure (Pr), pinch (Pi), and heat stimulation of the skin (grey boxes) recorded before (green) and after (red) IS. Profiles of heat stimulation show resting temperature (35 °C), stimulus temperatures (either 50 or 55 °C), and response thresholds (arrowheads). Numbers in parentheses indicate mean spikes/sec for pre-stimulus and stimulus intervals. Bin width: 500 msec.

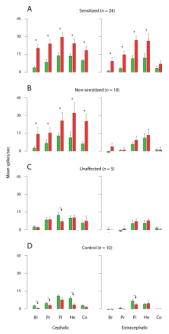

Fig. 3.

Mean ± SEM responses of thalamic units to brush (Br), pressure (Pr), pinch (Pi), heat (He) and cold (Co) stimuli applied to cephalic and extracephalic skin before (green) and after (red) exposing their dural receptive field to IS. Red bars represent the highest response magnitude recorded at any one time point after IS. Each bar represents the *net* neuronal firing invoked by a given stimulus, namely, mean firing rate during stimulation was corrected by subtracting the mean firing rate during a pre-stimulus interval (10 sec for mechanical stimuli; 30 sec for thermal stimuli). (*A*) Sensitized thalamic neurons increased their response magnitude to extracephalic brush ($p < 0.03$), pressure, pinch ($p < 0.001$) and heat ($p < 0.01$), and cephalic brush, pressure, pinch ($p < 0.005$), heat ($p < 0.01$) and cold ($p < 0.03$). (*B*) Non-sensitized thalamic neurons increased their response magnitude only to cephalic brush, pressure, heat, cold ($p < 0.02$) and pinch ($p = 0.05$). These neurons were considered to echo increased traffic of signals from sensitized trigeminovascular neurons of the SpV. (*C*) Unaffected thalamic neurons did not increase their responses to skin stimuli after IS (their response to cephalic pinch actually decreased; $p < 0.05$). (*D*) Control neurons, which were sham-stimulated with SIF at their dural receptive field, did not increase their responsiveness to any skin stimulation. Responses to certain stimuli (cephalic brush, pressure, heat; extracephalic pinch) actually decreased over time compared to baseline values ($p < 0.03$). Asterisks and downward arrows indicate significant difference between paired green and red bars (Wilcoxon test), as per the specific *P* values listed above.

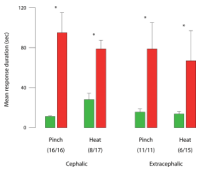

Fig. 4.

Prolonged responses of sensitized thalamic neurons to cephalic and extracephalic skin stimuli after exposing their dural receptive fields to IS. Bars represent mean ± SEM duration of activity bursts elicited by skin stimulation before (green) and after IS (red). Number of units exhibiting prolongation of response out of the total number of units tested is indicated in parentheses. Asterisks indicate significant difference between paired green and red bars (Wilcoxon test).

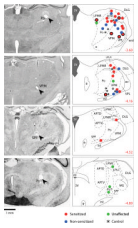

Fig. 5.

Localization of recording sites of trigeminovascular units in the rat posterior thalamus. Photomicrographs on the left show four examples of lesions marking the recording sites (arrow heads) in coronal sections stained with neutral red. Drawings on the right show the localization of all 49 units studied (one unit/rat) in coronal sections from the atlas of the rat brain by Paxinos and Watson's.[55] Numbers indicate the distance (in mm) relative to the Bregma point of reference. Units are color-coded into four groups according the key in the figure. Dots with solid borders represents sensitized units that started off with cutaneous receptive field restricted to the contralateral side of the face before IS. Abbreviations: 3V, third ventricle; APTD, anterior pretectal nucleus, dorsal; APTV, anterior pretectal nucleus, ventral; eml, external medullary lamina; DLG, dorsal lateral geniculate nucleus; fr, fornix; LDVL, laterodorsal thalamic nucleus, ventrolateral; LPLC, lateral posterior thalamic nucleus, laterocaudal; LPLR, lateral posterior thalamic nucleus, lateroorostral; LPMC, lateral posterior thalamic nucleus, mediorostral; LPMR, lateral posterior thalamic nucleus, mediorostral; MG, medial geniculate nucleus; ml, medial lemniscus; pc, posterior commissure; Po, posterior thalamic nucleus; PoT, posterior thalamic nucleus; SPF, subparafascicular thalamic nucleus; str, superior thalamic radiation; VPL, ventral posterolateral thalamic nucleus; VPM, ventral posteromedial thalamic nucleus.

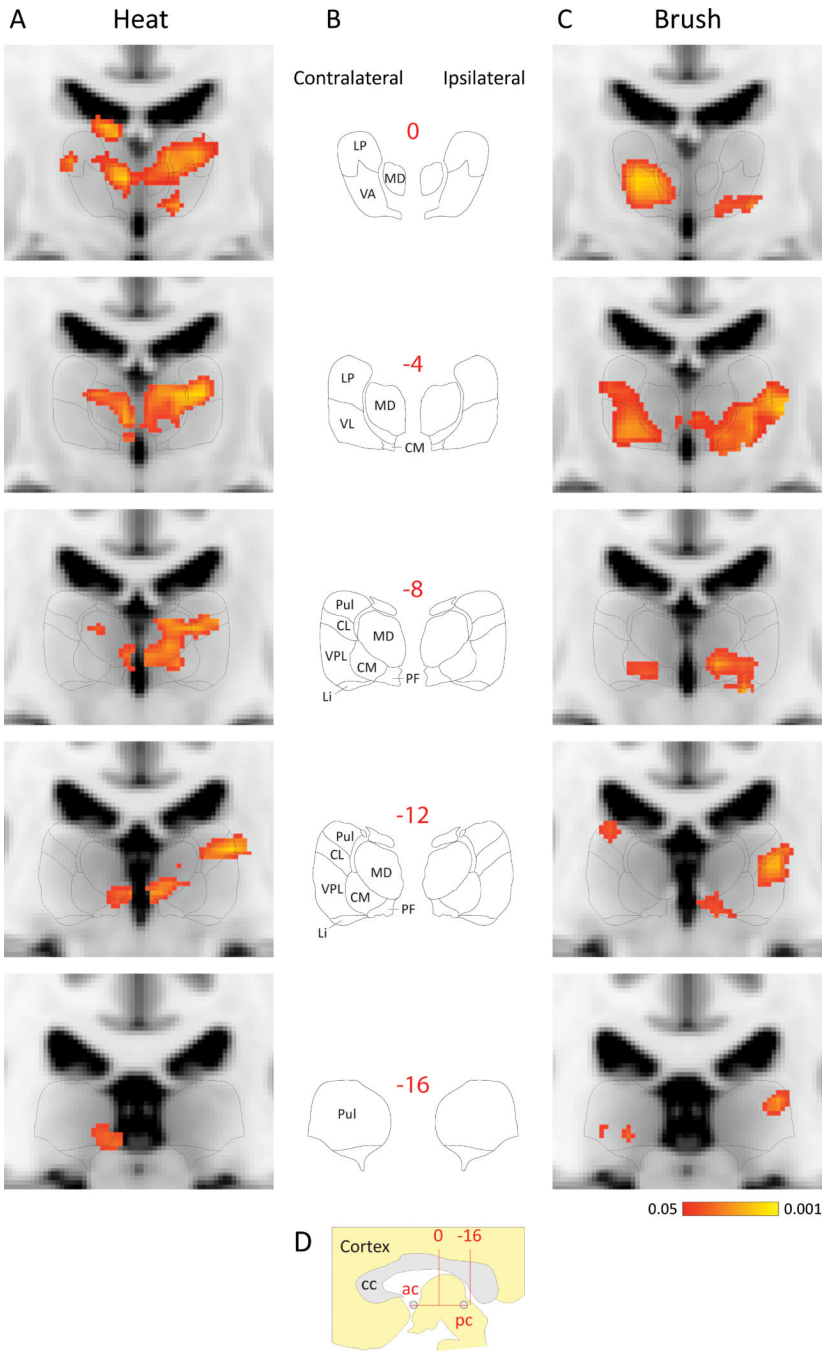

Fig. 6.

Contrast analysis of BOLD signals registered in fMRI scans of the human posterior thalamus following innocuous and noxious skin stimuli during migraine attacks that were associated with extracephalic allodynia. (*A*, *C*) Pooled statistical maps ($n = 8$) of responses to stimulation of the back of the hand using heat (*A*) and brush (*C*). Activation mapping probabilities are coded as indicated by the color bar at the bottom of *C*. (*B*) Drawings of the corresponding coronal planes (numbers in red) traced from Schaltenbrand and Wahren's atlas of the human brain.[31] (*D*) A sagittal perspective of the area of interest. Anterior-posterior coordinates (red numbers in *B*, *D*) indicate distance in mm from the midpoint (arrow in *D*) between the anterior and posterior commissures. BOLD signals were pooled

according to their ipsilateral/contralateral position in relation to the side of the headache (this normalized orientation is indicated at the top of *B*). BOLD signals were fitted onto MNI standard brain images, using FSL Linear Registration Tool (FLIRT). Schematic atlas drawings were size-fitted onto the corresponding MNI images to facilitate anatomical localization of BOLD signals. Abbreviations: ac, anterior commissure; cc, corpus callosum; CL, centrolateral thalamic nucleus; CM, centromedian thalamic nucleus; LI, limitans nucleus; LP, lateral posterior thalamic group; MD, mediodorsal thalamic group; pc, posterior commissure; PF, parafascicular thalamic nucleus Pul, pulvinar; VA, ventral anterior thalamic nucleus; VL, ventral lateral posterior thalamic group; VPL, ventral posterior lateral thalamic nucleus.